

A.Sh.Syzdykova¹, E.N.Eremin², S.A.Guchenko³, V.M.Jurov³¹«Kazakhmys» Corporation Polytechnic College, Balkhash;²Omsk State Technical University, Russia;³Ye.A.Buketov Karaganda State University

(E-mail: aigul.syzdikova@gmail.com)

Structure and properties of steel coating ligated zirconium

The paper presents experimental results on the structure and properties of coatings obtained while spraying a zirconium cathode and cathode steel 12X18H10T. The coatings were deposited in an atmosphere of nitrogen to the substrate 45. The coating of steel 12X18H10T + Zr in a nitrogen gas atmosphere has a high zirconium content of 3 times the iron content and the nitrogen content is 4. 12X18H10T + Zr coating in a gas atmosphere of argon and nitrogen have a columnar structure characteristic of single-phase films. To explain the observed structures are considered two mechanisms: the mechanism of concentration supercooling and the mechanism of propagation of dislocations due to the occurrence of thermal stresses in the coating. In the first step of coating thermal stresses do not have time to develop and the main role is making mechanism concentration supercooling, and in the second stage — both mechanisms.

Key words: multi-phase coating, x-ray analysis, microstructure, nanostructure, microhardness, nanohardness.

Introduction

At the present stage of development of mechanical engineering, including mining and oil, metal-working equipment effectiveness is largely dependent on the performance of cutting tools. One of the most effective methods of increasing the efficiency of the cutting tool is to apply its surface wear-resistant coatings [1, 2].

The first cutting inserts coated appeared on the foreign market in 1968, when the Swedish company «Sandvik Koromant» was developed and put into production a method of deposition of titanium carbide to carbide tools. In 1971, the company Teledyne Firth Sterlig (USA) have been received from the titanium nitride coating. In the Moscow Institute of Steel and Alloys in 1971 it developed a method for depositing a coating of niobium carbide.

In subsequent years, researchers in many countries (USA, France, Japan, Britain, Germany, etc.) Developed the technology application of various coatings for various applications. However, technology is not revealed in the press, and not published. Most foreign firms followed the way of providing services for the sale without coating technologies.

The most widely used in the industry find monolayer singletons wear-resistant coatings. However, in some cases, the efficiency of such an instrument is insufficient. In recent years, the interest of researchers has shifted to producing multi-layer and multi-element surfaces.

This paper presents the results of research of multi-coatings obtained by ion-plasma method.

The structure and properties of thin films comprising zirconium

Zirconium nitride were investigated in many studies, of which we mention the work [3–5]. Figure 1 shows a cross-section of the film ZrN, deposited on a substrate made of stainless steel AISI 316. There is a columnar structure. Nanoindentation results [3] showed that the hardness of the film is not related to its thickness. The thickness of the film significantly affect its roughness, grain size and electrical resistance.

Figure 2 shows an AFM image of the coating ZrN, obtained by reactive magnetron sputtering. There are 3 phases of zirconium nitride ZrN, Zr₃N₄ and ZrN₂. With increasing nitrogen partial pressure prevails education phase ZrN.

In [6] we investigated the coating Zr–Cu–N, representing the new material type metal nitride coating nanocrystalline (nc-MeN) / metal. The cut of the coating is shown in Figure 3, which shows that in this case, a columnar structure. The copper content of such coatings is about 2 at.%. But this leads to high elasticity coatings equal to about 80 %. The microhardness of the coating is about 40 GPa.

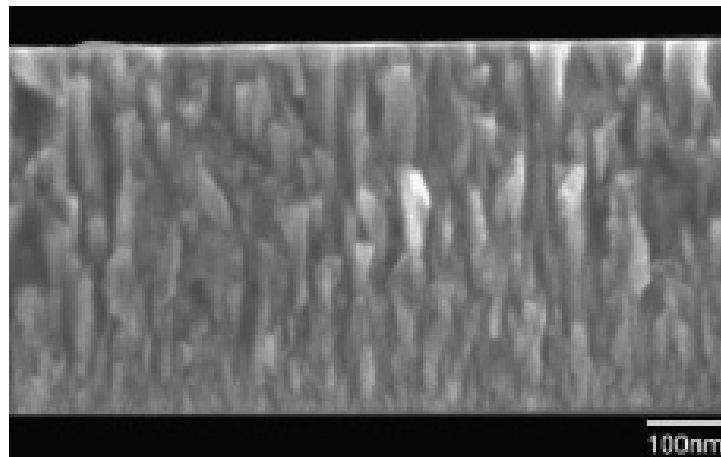


Figure 1. Slice ZrN coating structure [3]

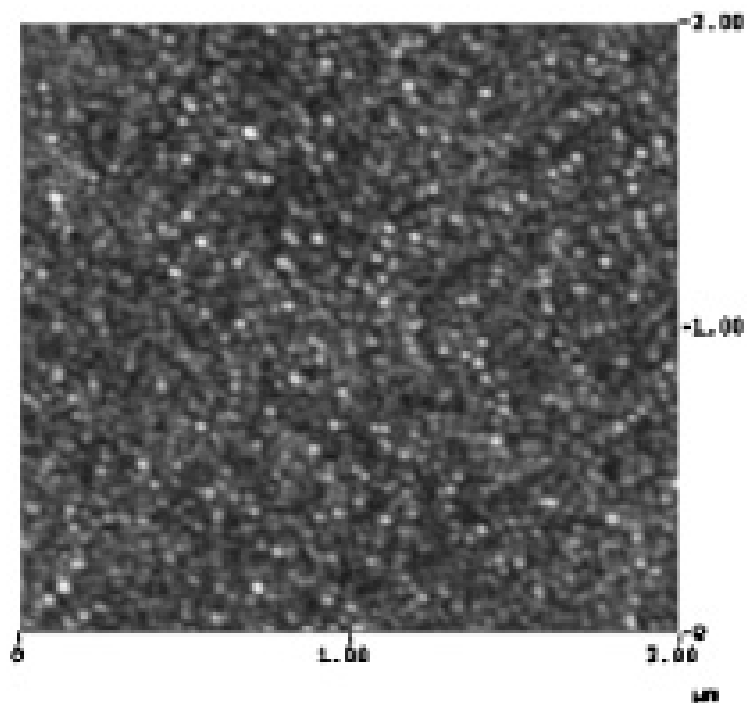


Figure 2. AFM images ZrN [5]

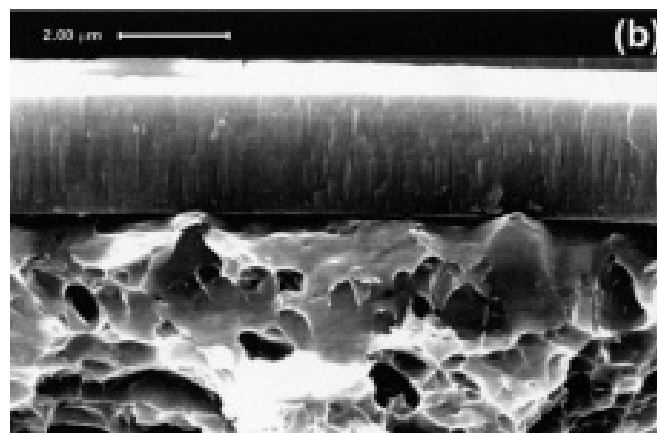


Figure 3. Slice coating Zr-Cu-N [6]

In [7] studied the properties of coatings $Zr_{1-x}Al_xN$. It is shown that there is an fcc structure. Education hcp structures characteristic of AlN, Here, there does not occur.

In [8, 9] investigated the coating Zr–Ni–N, obtained by magnetron sputtering target. It was found that the increase in hardness occurs in two cases (Fig. 4): (1) a material consisting of a mixture of fine grains of different crystallographic orientations, and (2) a material consisting of nanocolumns perpendicularly film / substrate interface.

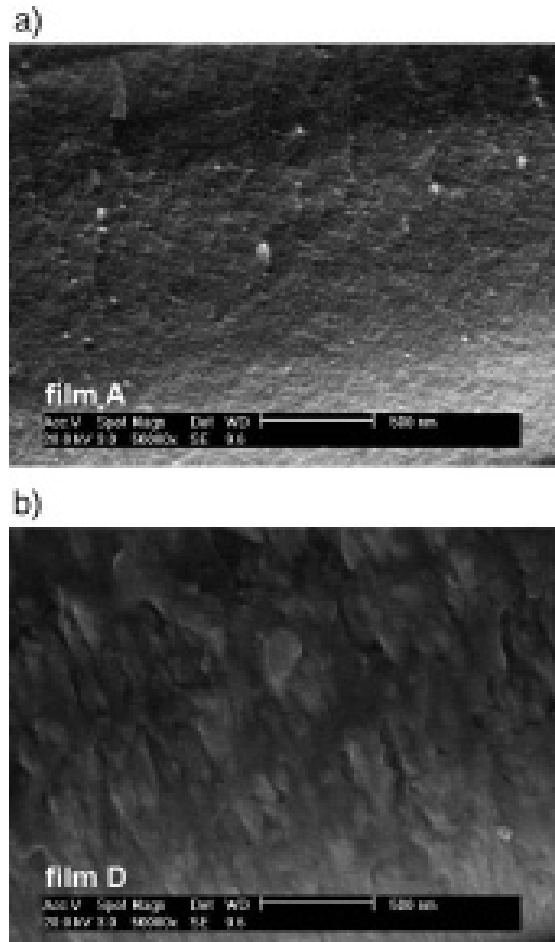


Figure 4. Electron microscopy image of two types of films Zr–Ni–N [9]

They were investigated and other types of coatings with zirconium: Zr–Ti–Cu–N [10], Zr–Y–N [11], Zr–Si–N [12], and others. In most cases, the hard coatings obtained with a microhardness of more than 40 GPa and having a grain size less than 20 nm.

Objects and methods of the experiment

The coating used zirconium cathodes and cathodes made of steel 12X18H10T. With these applied coatings to cathodes installation HHB steel for steel substrate 45 in a gas atmosphere of argon and nitrogen for 40 minutes at a current of $I = 80$ A, the reference voltage $V = 200$ V and a gas pressure in the chamber $P = 5 \cdot 10^{-3}$ Pa.

Electron microscopic study was conducted by a scanning electron microscope MIRA 3 firms TESCAN. The optical microstructure was investigated on metallographic microscope Epikvant, but at the nanoscale an atomic force microscope NT-206. By mathematical processing of energy-dispersive spectra of a special program PHI-RHO-Z were determined concentrations of elements.

Experimental results

Figures 5 and 6 show the AFM images of the coatings obtained in argon and nitrogen. Figure 7 shows an electron-microscopic image of argon and nitrogen.

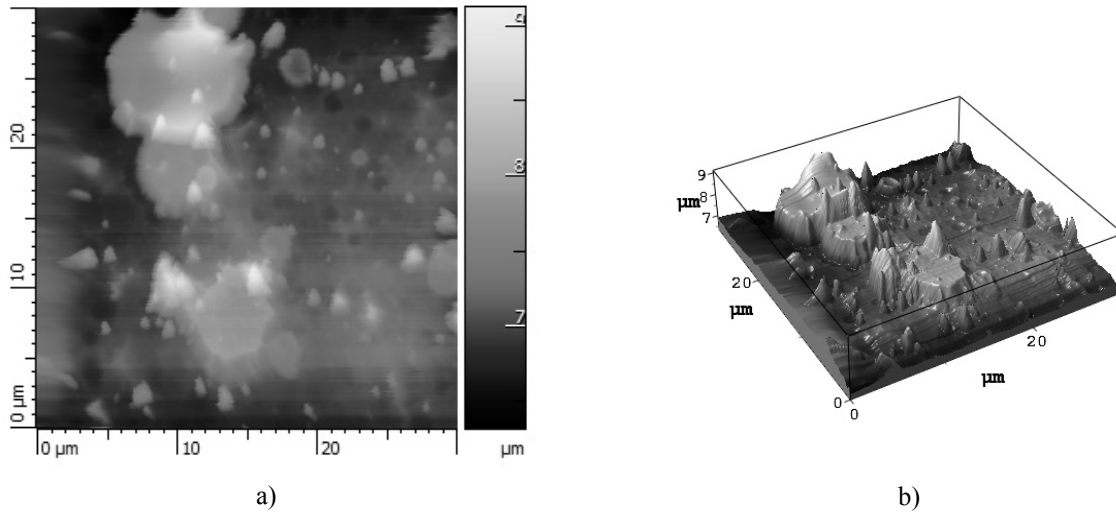


Figure 5. AFM image of the coating 12X18H10T + Zr in 1D (a) and 3D (b) projections of argon

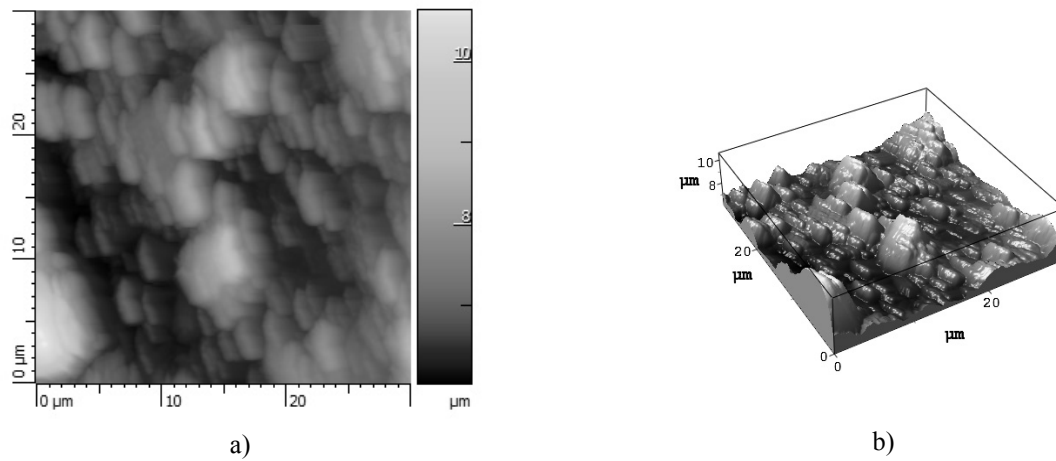


Figure 6. AFM image 12X18H10T + Zr coating in 1D (a) and 3D (b) under nitrogen projections

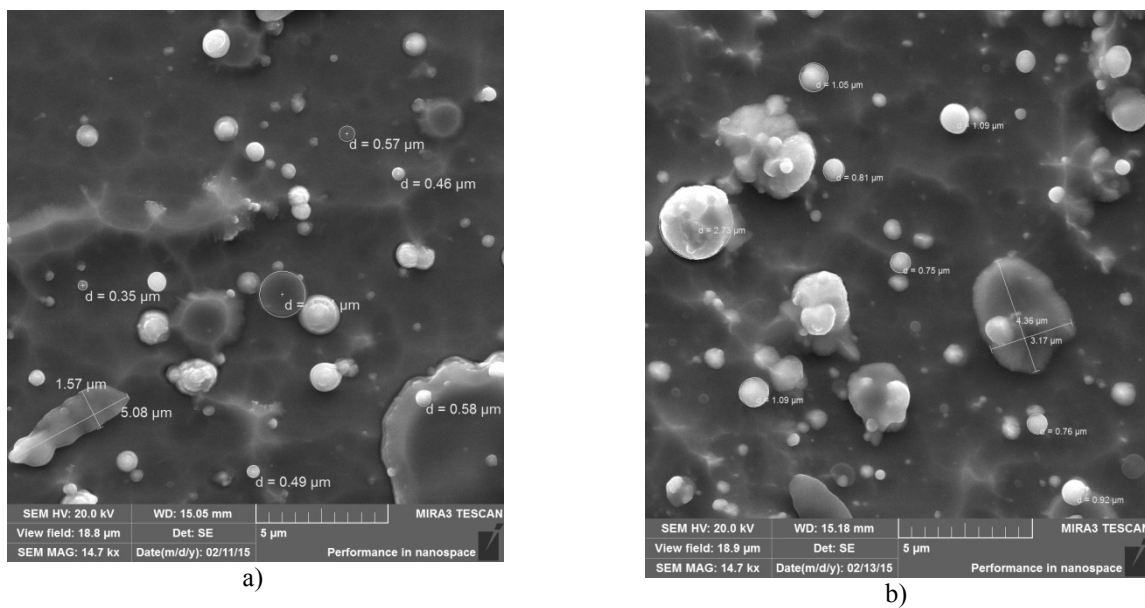


Figure 7. REM-cover image 12X18H10T + Zr in an argon atmosphere (a) and nitrogen (b)

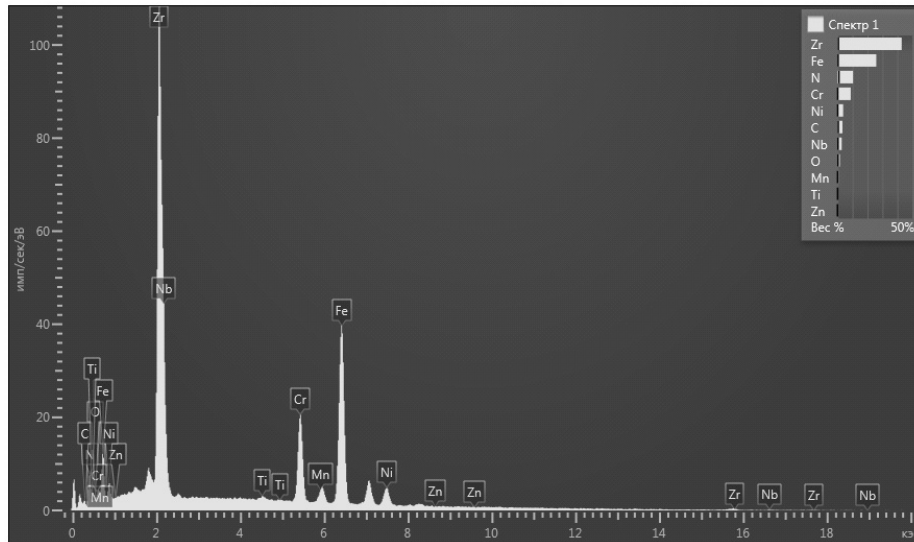


Figure 8. XPS 12X18H10T+Zr coating in nitrogen

Tables 1 and 2 show the elemental composition of the coatings in its two points of the experimental data of XPS (Fig. 8).

Table 1

The elemental composition of the coating 12X18H10T + Zr in nitrogen

| Element | Line type | Conventional concentration | The ratio k | Weight. % | Sigma weight % |
|---------|-----------|----------------------------|---------------|-----------|----------------|
| C | K series | 1.43 | 0.01433 | 3.28 | 0.48 |
| N | K series | 30.10 | 0.05358 | 10.36 | 0.98 |
| O | K series | 2.71 | 0.00913 | 1.56 | 0.31 |
| Ti | K series | 0.71 | 0.00713 | 0.23 | 0.06 |
| Cr | K series | 28.94 | 0.28939 | 8.77 | 0.17 |
| Mn | K series | 2.25 | 0.02247 | 0.70 | 0.10 |
| Fe | K серия | 83.77 | 0.83775 | 25.82 | 0.39 |
| Ni | K серия | 11.91 | 0.11912 | 3.69 | 0.15 |
| Zn | K серия | 0.00 | 0.00000 | 0.00 | 0.00 |
| Zr | L серия | 118.27 | 1.18270 | 42.84 | 0.61 |
| Nb | L серия | 7.94 | 0.07940 | 2.75 | 0.33 |
| Amount | | | | 100.00 | |

Table 2

Elemental composition of the coating 12X18H10T + Zr in nitrogen (another point)

| Element | Line type | Conventional concentration | The ratio k | Weight. % | Sigma weight % |
|---------|-----------|----------------------------|---------------|-----------|----------------|
| N | K series | 35.23 | 0.06272 | 12.53 | 0.82 |
| Ti | K series | 0.76 | 0.00759 | 0.26 | 0.06 |
| Cr | K series | 28.24 | 0.28243 | 9.00 | 0.16 |
| Mn | K series | 2.65 | 0.02652 | 0.87 | 0.10 |
| Fe | K series | 75.61 | 0.75606 | 24.37 | 0.31 |
| Ni | K series | 10.36 | 0.10359 | 3.34 | 0.15 |
| Zn | K серия | 0.00 | 0.00000 | 0.00 | 0.00 |
| Zr | L серия | 131.76 | 1.31757 | 49.63 | 0.54 |
| Amount | | | | 100.00 | |

The table shows a high zirconium content of 3 times the iron content and the nitrogen content is 4.

Discussion of the results of the experiment

Figures 5 and 6 show that the formation of ion-plasma coating formed honeycomb columnar structure. In the case of sputtering in nitrogen, film fills virtually the entire substrate and becomes more uniform. Figure 6 is quite similar to Figure 4. d cover Zr–Ni–N [9], wherein in the formation of the phase structure predominates ZrN_2 .

The formation of columnar structures is usually observed for single films (Fig. 1) and is described by the model proposed in [13]. In the presence of dopant, such a structure becomes globular, and is described by the model of Barna-Adamik [14].

However, in our case it is not realized neither one nor the other mechanism of the observed structure of the coatings. So we discuss this issue from the standpoint of self-ion-plasma coating represents an open system with distributed parameters.

Cellular columnar substructure is often formed during solidification as a result of occurrence of concentration supercooling (Fig. 9) [15]. If the formation of a cellular structure at the crystallization front there is a zone of liquid melt enriched impurity, the occurrence of segregation of impurities at the boundaries of the cells is required to lateral diffusion flux impurities from the top of the growing projection. The amount of impurity which does reach the cell boundary, it is difficult to measure, but it depends on the depth of the recess between the cells. As the hypothermia recess between the cells become deeper, which should lead to the enrichment of the cell border as a result of an admixture of impurity diffusion from the top of the cell. The concentration of impurities on the boundary can be several times higher than the concentration in the center of the cell.

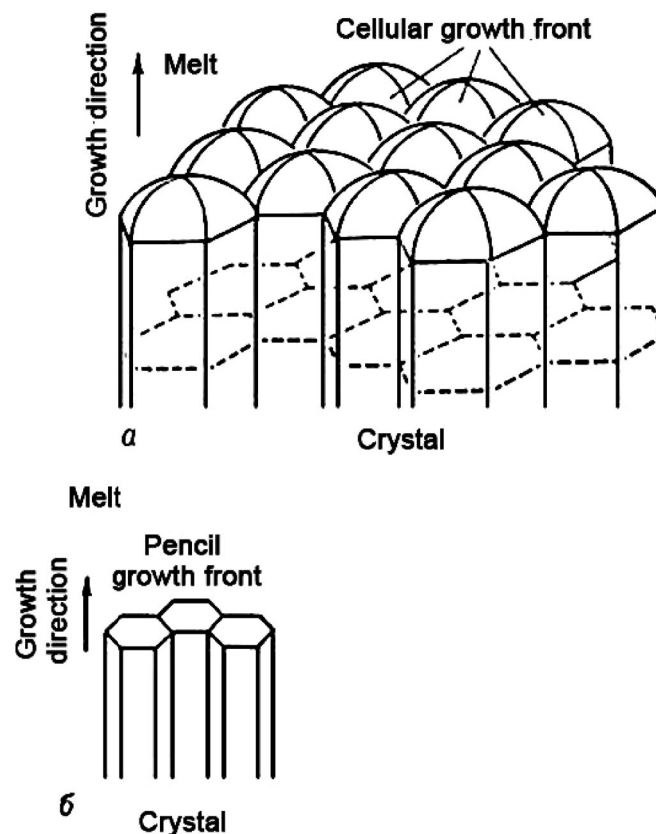


Figure 9. The cellular structure (a) and pencil (columnar) structure (b) [15]

Honeycomb structure consists of a series of parallel elements shaped as rods and arranged in the direction of crystallization (Fig. 9). The rods have a cross sectional shape of regular hexagons, and the structure at the solidification front is a collection of hexagonal cells. The upper surface of the free crystals having such a structure, wavy.

With further increase in thermal or concentration supercooling honeycomb structure is converted into dendritic. If you have a thermal melt supercooling (negative temperature gradient) any cell, was ahead of its

neighbors, starting to grow and develop more quickly, forming dendritic branches. This model is well suited to explain the observable cellular nanostructures, where the role played by the dopant zirconium nitride. However, there remains the question of why self-crystallizing the melt onto the surface of the substrate.

From the previous consideration of the formation of the structure of the ion-plasma coatings it shows that the situation is more complicated than it seems at first glance. In this section we will look at this issue from another angle, namely, using the model of cellular dislocation structure. Plastic deformation of crystals (and coatings), accompanied by the formation on the surface of strain relief, reflecting the process of localization of deformation in the crystal at the meso, micro and nanoscale level. Cellular dislocation structure begins to take shape in a deformed crystal at the end of the beginning of the third stage of strain hardening of metals and finishes at the end of the third stage (see. [16] and references therein). With further deformation of the material is formed fragmented dislocation structure (in the fourth and fifth stages of strain hardening). It is believed that cellular dislocation structure is a process of self-organization of dislocations in a multiple slip. For its origin is necessary to satisfy certain criteria (as in the case of Benard cells) linking multiplication factors, immobilization, and annihilation of dislocations. Modelled in [16] cellular dislocation structure is shown in Figure 10.

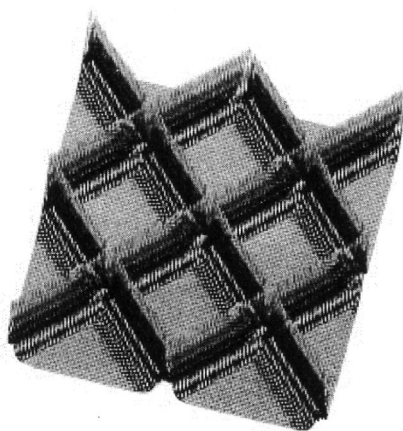


Figure 10. Cellular dislocation structure in perspective

In the process of ion-plasma coating and cooling of tensions generated in the last state [17], which can be a source of propagation of dislocations in the entire volume of the deposited coating. Observed with the sharp increase in the microhardness formed film is the result of dislocation hardening of the coating material. In a recent paper [18] a sharp increase in microhardness was observed in ion-plasma deposition high entropy alloys in a nitrogen atmosphere. However, the structure of the coating in this work was not investigated.

Closing

Although both these models qualitatively describe the experimental data presented in this paper, but the quantitative agreement with experiment is not. This is due to the fact that the proposed theory and contain a number of parameters that are difficult to define, and sometimes impossible.

References

- 1 Tabakov V.P., Chihranov A.V. Wear-resistant coating of cutting tools, working in continuous cutting. — Ulyanovsk: UISTU Publ., 2007. — 255 p.
- 2 Tabakov V.P. Formation of wear-resistant coatings ion-plasma cutter. — M.: Engineering, 2008. — 311 p.
- 3 Huang J.H., Yang H.C., Guo X.J., Yu G.P. Effect of film thickness on the structure and properties of nanocrystalline ZrN thin films produced by ion plating // Surface and Coatings Technology. — 2005. — Vol. 195. — P. 204–213.
- 4 Meng Q.N., Wen M., Qu C.Q. et al. Preferred orientation, phase transition and hardness for sputtered zirconium nitride films grown at different substrate biases // Surface and Coatings Technology. — 2011. — Vol. 205. — P. 2865–2870.
- 5 Rea M.D., Gouttebaron R., Dauchot J.-P. et al. Study of ZrN layers deposited by reactive magnetron sputtering // Surface and Coatings Technology. — 2003. — Vol. 174–175. — P. 240–245.
- 6 Zeman P., Cerstvy R., Mayrhofer P.H. et al. Structure and properties of hard and superhard Zr–Cu–N nanocomposite coatings // Materials Science and Engineering. — 2000. — Vol. A289. — P. 189–197.

- 7 Sheng S.H., Zhang R.F., Veprek S. Phase stabilities and thermal decomposition in the $Zr_{1-x}Al_xN$ system studied by *ab initio* calculation and thermodynamic modeling // *Acta Materialia*. — 2008. — Vol. 56. — P. 968–976.
- 8 Musila J., Karvankova P., Kasl J. Hard and superhard Zr–Ni–N nanocomposite films // *Surface and Coatings Technology*. — 2001. — Vol. 139. — P. 101–109.
- 9 Suna J., Musil J., Ondok V., Han J.G. Enhanced hardness in sputtered Zr–Ni–N films // *Surface and Coatings Technology*. — 2006. — Vol. 200. — P. 6293–6297.
- 10 Musil J., Danie R. Structure and mechanical properties of magnetron sputtered Zr–Ti–Cu–N films // *Surface and Coatings Technology*. — 2003. — Vol. 166. — P. 243–253.
- 11 Musil J., Polakova H. Hard nanocomposite Zr–Y–N coatings, correlation between hardness and structure // *Surface and Coatings Technology*. — 2000. — V. 127. — P. 99–106.
- 12 Daniel R., Musil J., Zeman P., Mitterer C. Thermal stability of magnetron sputtered Zr–Si–N films // *Surface and Coatings Technology*. — 2006. — Vol. 201. — P. 3368–3376.
- 13 Thornton J.A. Structure and topography of sputtering coatings // *Ann. Rev. Material Sci.* — 1977. — Vol. 7. — P. 239–260.
- 14 Barna P.B., Adamik M. Formation and Characterization of the structure of surface coating // *Protective Coatings and Thin Films* / Ed. Pfeau Y., Barna P.B. — Kluwer Academic, Dordrecht, The Netherlands, 1977. — P. 279–297.
- 15 Vayngard W. Introduction to the physics of crystallization metallo. — M.: Mir, 1967. — 170 p.
- 16 Maligin G.A. Modelling of deformation of the surface relief plastically deformable crystal // *FTT*. — 2007. — Vol. 49, № 8. — P. 1392–1397.
- 17 Barvinok V.A. Managing stress state and properties of plasma coatings. — M.: Engineering, 1990. — 384 p.
- 18 Sabol O.V., Andreev A.A., Gorban V.F. et al. On the reproducibility of single-phase structural state multielement hightentropy system Ti–V–Zr–Nb–Hf and high hard nitrides based on it as they are formed by vacuum arc method // *Technical Physics Letters*. — 2012. — Vol. 38, No. 13. — P. 40–47.

А.Ш.Сыздыкова, Е.Н.Еремин, С.А.Гученко, В.М.Юров

Циркониймен легирленген болат жабындысының құрылымы және қасиеттері

Мақалада 12X18H10T болат және циркон катодтары бір уақытта ыдырату кезінде алынған жабындының құрылымы мен қасиеттері бойынша эксперименталды нәтижелері келтірілген. Жабындылар 45 болат астына азоттың ортасында берілген. 12X18H10T+Zr жабындысына газды азоттың ортасында жоғары цирконий сипатында 3 есе жоғарлайтын темір және 4 азот сипаты тән. 12X18H10T+Zr жабындысы азот және аргон газды ортасында бірфазалық қабыршақ үшін бағаналық сипатқа ие. Байқалған құрылымның түсіндірмесі үшін екі тетік қарастырылады: концентрациялық суытылу тетігі және дислокацияның көбею тетігі есебіне қатысты термиялық кернеу жабындысы. Бас жабынды пайда болуының бірінші кезеңінде термиялық кернеулер дамуға үлгермейді және негізгі рөлді концентрациялы суыту тетігі енгізеді, ал екінші кезеңде — екі тетік те әрекет етеді.

А.Ш.Сыздыкова, Е.Н.Еремин, С.А.Гученко, В.М.Юров

Структура и свойства стальных покрытий, легированных цирконием

В работе приведены экспериментальные результаты по структуре и свойствам покрытий, полученных при одновременном распылении циркониевого катода и катода из стали 12X18H10T. Покрытия наносились в среде азота на подложку из стали 45. Покрытие 12X18H10T+Zr в газовой среде азота имеет высокое содержание циркония, в 3 раза превышающее содержание железа и в 4 — содержание азота. Покрытия 12X18H10T+Zr в газовой среде азота и аргона имеют столбчатую структуру, характерную для однофазных пленок. Для объяснения наблюдаемой структуры рассматриваются два механизма: механизм концентрационного переохлаждения и механизм размножения дислокаций за счет возникновения в покрытии термических напряжений. На первой стадии образования покрытия термические напряжения не успевают развиваться, и основную роль играет механизм концентрационного переохлаждения, а на второй стадии действуют оба механизма.